AIAA Modeling and Simulation Technologies Conference
2 - 5 August 2010, Toronto, Ontario Canada

AIAA 2010-8096

Effects of Visual Spatio-Temporal Aliasing on Pilot Performance in Active Control Tasks

Peter M.T. Zaal* and Barbara T. Sweet†
NASA Ames Research Center, Moffett Field, CA

Visual display systems such as the out-the-window or head-down displays of a simulator present a visual scene that is sampled in both the spatial domain (by the display resolution) and the time domain (by the display refresh rate). For a given human visual temporal sensitivity, spatial-frequency content of the scene, and speed of the image motion, spatio-temporal aliasing can occur when the image is sampled at a rate that is too low. The effects of spatio-temporal aliasing on visual perception are understood to some extend. However, not much is known about the effects on pilot performance in active control tasks. This paper presents the results of an experiment to determine the effects of spatio-temporal aliasing on pilot performance and control behavior in a target-tracking task. To induce different levels of spatio-temporal aliasing, the refresh rate of the experimental display was varied among five different levels. The results indicate that pilots adopt a different control strategy when the display refresh rate is increased from 60 to 120 Hz. The visual gain and neuromuscular frequency of the identified pilot model increase, while the visual time delay decreases. This change in control strategy allows for a higher tracking performance at higher display refresh rates as indicated by a decrease in root mean square of the error signal and an increase in crossover frequency.

Nomenclature

A_t	sinusoid amplitude
e	tracking error signal
f_t	target forcing function
$H(s)$	transfer function
$H(j\omega)$	frequency response function
K_v	visual gain
k	sinusoid index
N_t	number of sine waves
n_t	forcing function frequency integer factor
n	pilot remnant signal
r	image motion
s	Laplace variable
T_{A1},T_{A2}	forcing function filter time constants
T_{lead}	visual lead time constant
T_m	measurement time
t	time
u	pilot control signal
u_l	human spatial resolution limit
y	controlled system state

Symbols

ζ_{nm}	neuromuscular damping
σ	standard deviation
τ_v	visual time delay
ϕ_t	sinusoid phase shift
φ_m	phase margin
ω	frequency
ω_c	crossover frequency
ω_{cs}	critical sampling frequency
ω_l	human temporal resolution limit
ω_{nm}	neuromuscular frequency
ω_t	sinusoid frequency

Subscripts

c	controlled system
ol	open loop
p	pilot

*Ph.D. candidate, Control and Simulation Division, Faculty of Aerospace Engineering, Delft University of Technology, P.O. Box 5058, 2600GB Delft, The Netherlands; p.m.t.zaal@tudelft.nl. Student member AIAA.
†Aerospace Engineer, Human Systems Integration Division, NASA Ames Research Center, Moffett Field, CA, 94035; barbara.t.sweet@nasa.gov. Member AIAA.

I. Introduction

In flight simulation, many challenges exist in accurately simulating the outside visual scene from the simulator cockpit. Techniques have been developed to improve the quality of the static simulated visual scene. However, as aircraft move, the quality of the visual scene in motion should also be considered. When motion is introduced in a simulated visual scene, perceptual artifacts, such as motion induced blur and spatio-temporal aliasing, can become apparent.[1,2]

Spatio-temporal aliasing is associated with temporal sampling of a moving image and depends on both the refresh rate (temporal sampling) and the image resolution (spatial sampling). When a moving image is sampled at a refresh rate that is too low, spatio-temporal artifacts will become visible to the human observer and the sampled image will not be an accurate simulation of the original scene. Watson et al. proposed and experimentally validated a theory that predicts the visual conditions at which a human observer would be able to detect the refresh rate at which sampling becomes detectable.[3] For images with a less than eye-limiting maximum spatial frequency, the critical sampling frequency – that is, the frequency where aliasing becomes apparent – is found to be a function of human temporal sensitivity, speed of the image motion, and spatial resolution of the image. In previous experiments, the perception of spatio-temporal aliasing artifacts was studied in passive tasks.[3–5] These studies indicate that at higher image resolutions (for a given refresh rate), the visibility of spatio-temporal aliasing artifacts will occur at lower image velocities. Increasing the refresh rate of the display device reduces the visibility of these artifacts.

In a flight simulator most piloting tasks require pilots to utilize visual information displayed by the outside visual system or head-down displays. However, very little research has been performed to determine the effects of spatial-temporal aliasing on pilot performance in these tasks. Dearing et al. showed that the sink rate in an autorotative descent and landing of a Blackhawk helicopter was worse with a high resolution ground texture compared to lower resolution textures.[6] The highest resolution texture induced significant spatio-temporal aliasing compared to the lower resolution textures. It is hypothesized that the drop in performance was a result of impaired velocity perception caused by spatio-temporal artifacts.

The current study aims to provide more insight into the effects of spatio-temporal aliasing on pilot performance in an active control task. An experiment was conducted in which 10 general aviation pilots performed a target-tracking task, while the refresh rate of the CRT monitor displaying a compensatory display was varied across five different refresh rates. The spatial frequency of the stimulus and the speed of the stimulus motion were kept constant for every condition. With increasing refresh rate, spatio-temporal aliasing artifacts were less apparent and the stimulus motion appeared to be smoother. In addition to studying the effects on pilot performance, the impact on pilot control behavior was analyzed by estimating the parameters of a pilot model using the experimental data.[7]

This paper first gives a discussion on spatio-temporal aliasing and the consequences on human visual perception in Sec. II. Next, the experiment setup will be described in Sec. III, after which the results will be given in Sec. IV. The paper ends with a discussion and conclusions.

II. Spatio-Temporal Aliasing

Out-the-window and head-down displays of flight simulators present visual scenes that are sampled both spatially and temporally.[3] The spatial sampling rate is determined by the pixel frequency, or resolution, of the display device and the temporal sampling rate by its refresh rate. Aliasing occurs when the image is sampled using a sampling rate that is too low. A sampled signal that is periodic and contains frequencies above the Nyquist frequency – that is, half the sampling frequency – will typically exhibit frequency content that is different from the original signal. When aliasing occurs, a sampled image will not be an accurate recreation of the original scene and distortions and artifacts will become visible to the human observer.[2]

Figure 1 gives an example of aliasing in the time domain. In Figure 1a, a sinusoidal signal with a fundamental frequency of 1 Hz is depicted. The sampling frequency is 100 Hz, which implies that the Nyquist frequency is 50 Hz. No aliasing occurs, as the fundamental frequency of the sine wave is well below the Nyquist frequency. Figure 1b depicts the same sine wave, but now with a sampling frequency of 1.2 Hz. This means the fundamental frequency of the sine wave is now higher than the Nyquist frequency of 0.6 Hz, resulting in significant aliasing. The reconstructed signal is not an accurate recreation of the original signal and appears to have a different, much lower fundamental frequency than the original signal.

An example of spatial aliasing is shown in Figure 2. Figure 2a depicts a texture of a sinusoidal grating

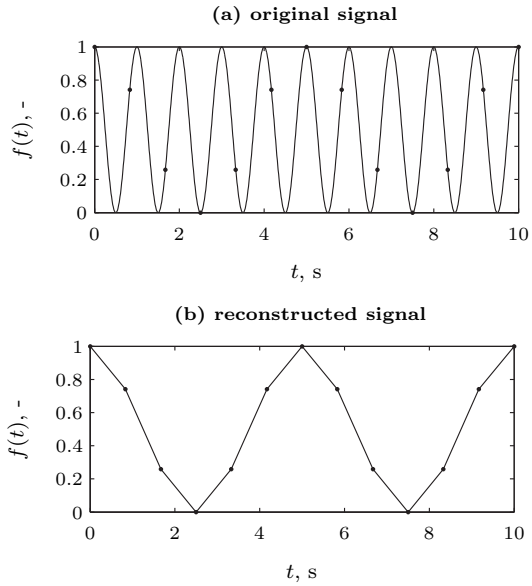

Figure 1. Temporal aliasing.

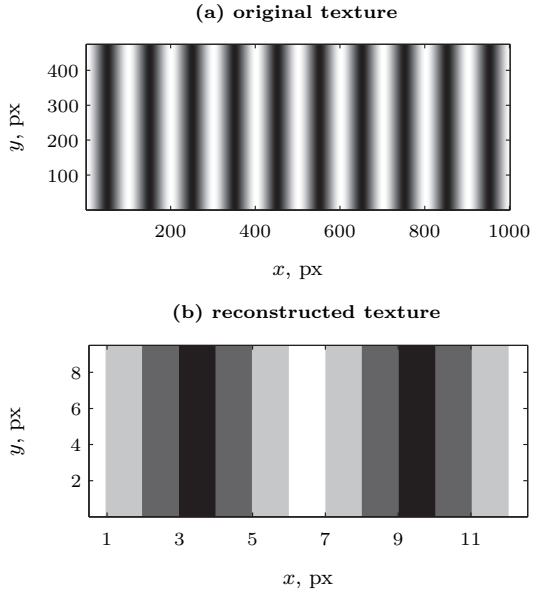

Figure 2. Spatial aliasing.

with a fundamental frequency of 0.01 cycles/px. This fundamental frequency is much lower that the Nyquist frequency of 0.5 cycles/px. The same texture is depicted in Figure 2b, but with a much lower spatial resolution. In this case the fundamental frequency is 0.83 cycles/px, higher than the Nyquist frequency of 0.5 cycles/px. The reconstructed texture appears to be very different from the original texture. Note that for clarification, both the temporal and spatial aliasing examples are constructed using the same sine wave, that is, when not taking into account the units on the x- and y-axis, Figure 1 can be considered a cross section of the texture in Figure 2.

Spatio-temporal aliasing is related to the temporal sampling of an image in motion. A well-known example is the wagon-wheel effect. In a sequence of camera images of a spoked wheel rotating more than half of the angle between the spokes per frame, the rotational motion of the wheel is perceived in the direction opposite of the original direction. Although this is a special case of a repeating visual image due to the symmetry of the wheel, spatio-temporal aliasing can occur with any image sequence depending on the sampling rate and image resolution.

In previous research, an analytical method was developed to predict when human observers can detect spatio-temporal aliasing.[3] The theory states that the critical sampling frequency – that is, the frequency where aliasing artifacts become apparent – is a linear function of the image speed:

$$\omega_{cs} = \omega_l + r u_l \tag{1}$$

with ω_{cs} the critical sampling frequency, r the image speed, and u_l and ω_l the human limits of spatial and temporal resolution, respectively. This linear relation was experimentally validated in a two-interval forced-choice experiment where subjects had to distinguish a smoothly moving line from a line that was sampled at a certain refresh rate. The critical sampling frequency was determined for six different image speeds between 0 and 20 deg/s. The data from two subjects participating in the experiment and the linear data fits are depicted in Figure 3. An increase in critical sampling frequency can be observed for an increase in image motion speed. Note that the spatial resolution limit is almost equal for both subjects (30 and 33 Hz), but the temporal resolution limit is significantly different (6 and 13 cycles/deg).

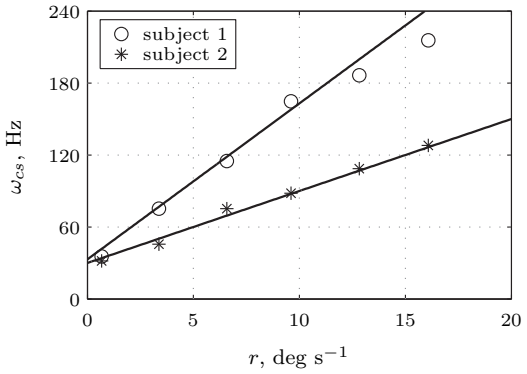

Figure 3. Critical sampling frequency for stroboscopic motion as a function of velocity for two subjects. The data is taken from Watson et al.[3]

Although the data in Figure 3 supports the theory of a linear relationship between critical sampling

frequency and image motion speed, the estimates of the human limits of spatial and temporal resolution are thought to be too low for both subjects. This can mainly be explained by the fact that the analysis is based on the discrimination between sampled and continuous motion, not on assessing when spatio-temporal artifacts become noticeable, distracting or impact task performance. However, the data still gives some indication of a lower estimate of the monitor refresh rate required to eliminate spatio-temporal artifacts for a given speed of a moving line. For a full moving image – with a wide range of spatial frequency components – known non-linear interactions across frequency components, such as masking, exist. These interactions are not reflected in the results depicted in Figure 3.

III. Experiment

A. Method

1. Active Control Task

To study the effects of spatio-temporal aliasing on pilot performance and control behavior in an active control task, pilots performed a target-tracking task, minimizing the error e between a target signal f_t and the controlled system output y. This task is depicted in Figure 4. The error between the target and system output was visualized by the distance between two vertical lines on a compensatory display, see Figure 5. In this type of control task, the pilot can be modeled by a linear response function H_p and a remnant signal n that accounts for nonlinearities in the pilot's output.

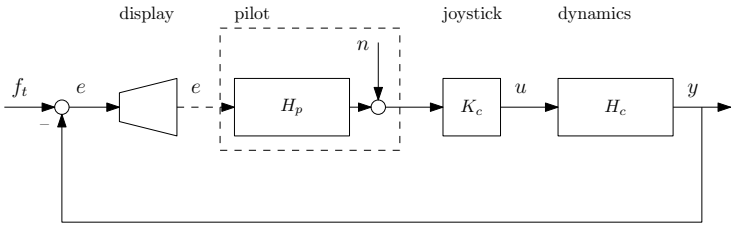

Figure 4. Closed-loop control task.

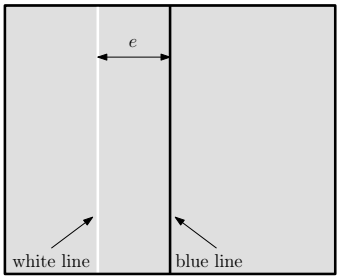

Figure 5. Compensatory display.

The pilots in this study provided control inputs u to the controlled dynamics using left-right deflections of a joystick with a gain $K_c = 3$. The controlled dynamics H_c were given by:

$$H_c(s) = \frac{600}{s(s + 0.2)} \tag{2}$$

These dynamics resemble single-integrator dynamics below a frequency of 0.2 rad/s and double-integrator dynamics above this frequency. According to the principles of McRuer's crossover theorem, these controlled dynamics require the pilot to generate lead at frequencies above 0.2 rad/s to compensate for the double-integrator dynamics around the crossover frequency.[7]

To measure skill-based pilot control behavior, a randomly appearing multi-sine signal was used as the target signal. The signal was a sum of twelve independent sine waves generated using the following equation:

$$f_t(t) = \sum_{k=1}^{N_t} A_t(k) \sin[\omega_t(k)t + \phi_t(k)] \tag{3}$$

with $N_t = 12$ the number of sine waves, and ω_t, A_t and ϕ_t the frequency, amplitude and phase shift of the k^{th} sine wave, respectively. The measurement time of an individual experiment measurement run was $T_m = 68.267$ s. With a total run length of 90 s and data logging at 120 Hz, this is the largest measurement time with a power of two data points ($2^{13} = 8192$). The sinusoid frequencies $\omega_t(k)$ were all integer multiples of the measurement time base frequency, $\omega_m = 2\pi/T_m = 0.0767$ rad/s, and were selected to cover the frequency range of human control.

A second-order low-pass filter was used to determine the amplitudes of the individual sines:

$$H_A(j\omega) = \left(\frac{1 + T_{A1} j\omega}{1 + T_{A2} j\omega}\right)^2 \tag{4}$$

with $T_{A1} = 0.1$ s and $T_{A2} = 0.8$ s. The absolute value of the filter at a sinusoid frequency gives the corresponding sinusoid amplitude. The reduced magnitude of the amplitudes at higher frequencies yields a tracking task that is not overly difficult.[8] The amplitude distribution was scaled to attain a target forcing function with a standard deviation of 100 px. Given the display resolution, the dimensions of the screen, and a viewing distance of 2 ft, this is equivalent to a visual angle of 3.763 deg.

To determine the forcing function phase distribution, a large number of random phase sets were generated. The set that yielded a signal with a probability distribution closest to a Gaussian distribution, without leading to excessive peaks, was selected.[9] The final forcing function properties used in the experiment are summarized in Table 1. A time trace of the target signal is given in Figure 6. The y-axis in the figure indicates degrees of visual angle at a viewing distance of 2 ft.

Table 1. Forcing function properties.

k, –	n_t, –	ω_t, rad s^{-1}	A_t, px	ϕ_t, rad
1	6	0.552	91.986	-2.571
2	9	0.828	76.683	-1.059
3	13	1.197	58.017	1.736
4	19	1.749	38.198	2.060
5	27	2.485	23.499	-2.790
6	41	3.774	12.381	-1.221
7	53	4.878	8.361	2.020
8	73	6.719	5.322	0.127
9	103	9.480	3.556	1.483
10	139	12.793	2.733	-0.537
11	194	17.856	2.239	-1.675
12	229	21.077	2.091	-2.230

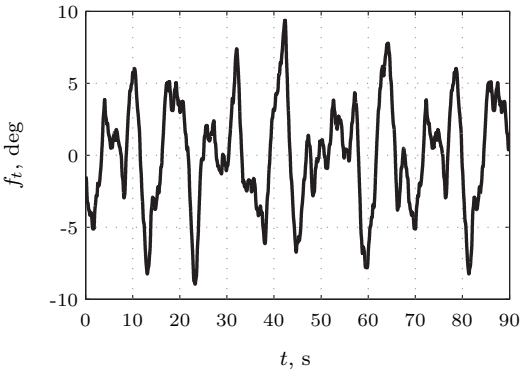

Figure 6. Target forcing function time trace.

2. Independent Variables

For a given human temporal sensitivity, the visibility of aliasing depends on the refresh rate of the display, the maximum spatial frequency of the image, and the velocity of the image motion. Only one independent variable was varied in this experiment: display refresh rate. Five different conditions were performed where the refresh rate of the CRT monitor was either 60, 75, 90, 105 or 120 Hz. The maximum spatial frequency of the visual stimulus was constant during the experiment. The velocity of the stimulus is dictated by the derivative of the target forcing function defined in the previous section and the control strategy of the pilot. Although the velocity varies over time, implying that the intensity of the spatio-temporal artifacts varies over time, this variable can also be considered a constant between runs if the pilot adopts a consistent control strategy.

3. Apparatus

The experiment was performed at one of the vision labs of NASA Ames Research Center. The lab was completely blacked out; that is, no outside light could enter the room and the walls were covered in black fabric to reduce light reflections.

The experiment computer was equipped with a NVIDIA Quadro FX 5500 video card and was running a Linux operating system. The experiment software was updating and logging data at 120 Hz, that is, at the highest monitor refresh rate used in the experiment.

The compensatory display shown in Figure 5 was depicted on a ViewSonic G225f CRT monitor. This monitor has a display area with a width of 410 mm and a height of 300 mm; that is, the viewable diagonal area was 20 inch. Pilots were seated 2 ft from the CRT monitor, which means the total horizontal field of view was 37.17 deg. During the experiment the resolution of the screen was set to 1024x768 px. The width of both lines of the compensatory display was 2 px or 0.075 deg of visual angle. At the start of each experimental run, the refresh rate of the screen was changed using the display driver. Vertical synchronization (v-sync) was turned on; that is, the frame changes were synchronized to the vertical blanking interval of the CRT.

Pilots provided control inputs using left-right movements of a joystick (Logitech Extreme 3D Pro). This right-handed joystick had a considerable breakout force. Pilots could rest their right arm on an armrest. A stick gain of 3 was used, which means that joystick displacement values ranged from -3 to 3, corresponding to full left and right deflections, respectively.

4. Participants and Instructions

Ten general aviation pilots participated in the experiment. All pilots were male and between 28 and 41 years old. The average total of flying hours was 3633 with an average of 128 flying hours in the previous six months. Two of the pilots were left handed, but were comfortable giving control inputs with their right hand. None of the pilots were familiar with the type of control task used in this experiment.

Every pilot received a briefing before the start of the experiment. The briefing contained information about the objective, control task and procedures of the experiment. The pilots were also informed about the fact that there would be five different experimental conditions in which the refresh rate would vary. However, the specifics of the conditions were not provided. Pilots were instructed to focus on the middle of the CRT monitor during the experiment. The main instruction was to minimize the error presented on the visual display as best they could.

5. Procedures

Every experiment run had a length of 90 s. For the first 21.733 s pilots were able to stabilize the controlled dynamics and adjust to the task. Data from these first 21.733 s were discarded for analyses and only data from the last 68.267 s were used as measurement data (see Sec. III.A.1).

During the experiment, the pilot's tracking performance – defined as the root mean square (RMS) of the error signal – was recorded for every run. To motivate the participating pilots to perform at their maximum level of performance, they were informed of the best overall performance across pilots and their own performance after each run.

The experiment had a balanced Latin-square design; that is, the conditions were presented in a quasi-random order. Pilots were not informed about which condition they were performing. A total of 16 runs were performed for each condition of which the first 4 were considered training runs. After these first 4 runs, the experimenter made sure the pilot reached asymptotic performance; that is, attained more or less constant values of the RMS of the error. The last 8 recorded runs for each condition were used for the final data analysis.

Typically, each pilot performed 20 runs between breaks. However, they were encouraged to take a break when feeling any discomfort. Every pilot was able to complete the experiment within 4 h.

6. Dependent Measures

A number of dependent measures were considered to be of interest for this experiment. First, the performance and control activity of the pilots in the target tracking task were evaluated in terms of the RMS of the error and control signals, respectively. In addition, the pilot frequency response function H_p (see Figure 4) was identified and parameterized using McRuer's precision model.[10] The estimated pilot model parameters allow for a quantitative analysis of the effects of spatio-temporal aliasing on pilot control behavior. The linear describing function of the precision model is given by:

$$H_p(s) = K_v(1 + T_{lead}s)e^{-\tau_v s}\frac{\omega_{nm}^2}{\omega_{nm}^2 + 2\zeta_{nm}\omega_{nm}s + s^2} \tag{5}$$

with K_v the visual gain, T_{lead} the visual lead time constant, τ_v the sum of the perceptual and motor delays that specify the pilot's equivalent reaction time, and ζ_{nm} and ω_{nm} the neuromuscular damping and frequency, respectively. All these parameters are estimated in the pilot model optimization process.

Finally, the effect of the changes in control behavior on the attenuation of the target signal was evaluated from the open-loop response. In the frequency domain, pilot performance is determined by the crossover frequency and phase margin of the open-loop response. Using the identified pilot response functions and the controlled dynamics [Eqs. (2) and (5)], the open-loop response is determined by:

$$H_{ol}(s) = H_p(s)H_c(s) \tag{6}$$

The crossover frequency ω_c, is the frequency where the magnitude of the open-loop response crosses the line with a magnitude of 1. The corresponding phase margin φ_m is the phase difference with -180 deg at the crossover frequency.

B. Hypotheses

Previous experiments on the effects of spatio-temporal aliasing mainly investigated the effects on visual perception in passive tasks.[3] However, there is not much known about the effects of these artifacts on pilot performance in active control tasks. Various experiments have been conducted that demonstrated that visual motion perception was compromised, that is, less lead was generated by the pilot, when visual features such as contrast and color were degraded.[11,12] It has been suggested that spatio-temporal aliasing has the same effect on pilot performance and control behavior.[13]

Therefore, the main hypothesis of this study is that spatio-temporal aliasing will compromise the pilot's ability to generate lead. When the refresh rate of the screen decreases, the artifacts become more apparent, and the visual lead time constant of the pilot model will decrease. Furthermore, it is hypothesized that the visual time delay will increase for decreasing refresh rates. With fewer screen updates per second, more time is needed to process the visual information. An increase in visual time delay when visual information content is degraded has also been shown in previous experiments.[14]

These changes in pilot control strategy will be reflected in the pilots' tracking performance as determined by the RMS of the error signal. It is hypothesized that for decreasing refresh rates, performance will degrade. In the frequency domain the degradation in performance will be observed by a decrease in crossover frequency.

IV. Results

This section presents the combined results of the 10 general aviation pilots who performed in the experiment. For every subject and every condition the data are averaged over eight runs. The error bars in the error bar plots are corrected for between-subject variability by normalizing the subject means across conditions.[15] All the data are analyzed using a repeated-measures analysis of variance (ANOVA) to uncover any significant trends. Mauchly's test of sphericity indicated that the assumption of sphericity was met ($p > 0.05$) for all the ANOVA results and no correction of the data was needed.

A. Tracking Performance and Control Activity

Tracking performance and control activity are evaluated using the RMS of the error and control signals, respectively. Figure 7a depicts the RMS of the error signal. It can be observed that the RMS of the error decreases – that is, performance improves – for higher CRT monitor refresh rates. The ANOVA indicates that this effect is highly significant [$F(4, 36) = 15.857$, $p < 0.001$]. The data show a linear trend across the conditions that explains 96% of the variance, as is indicated by polynomial contrasts [$F(1, 9) = 51.984$, $p < 0.001$].

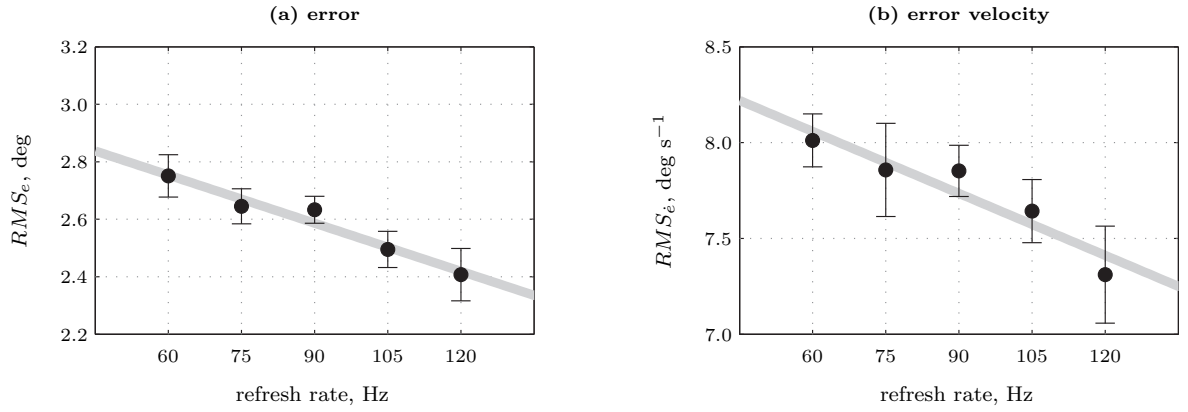

Figure 7. Means and 95% confidence intervals of the RMS of the error and error velocity. The data are corrected for between-subject variability. Significant linear trends are indicated by grey lines.

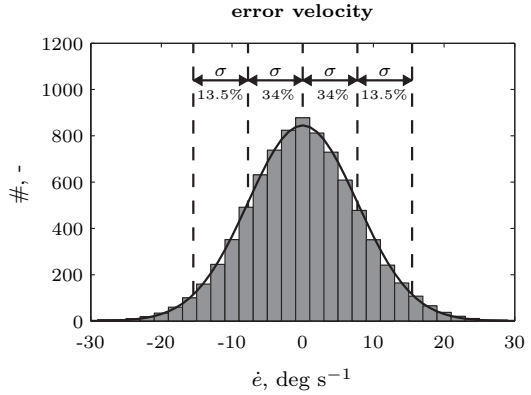

Figure 8. Mean histogram and normal distribution approximation of the error velocity.

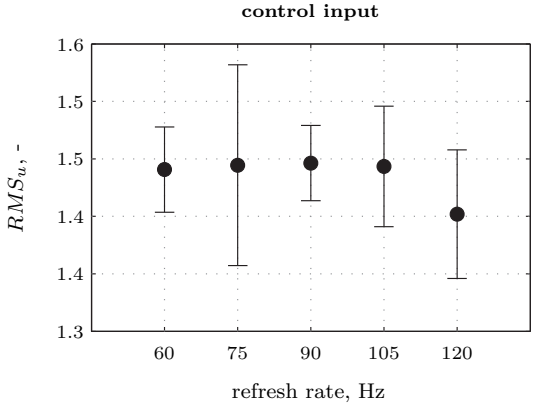

Figure 9. Means and 95% confidence intervals of the RMS of the pilot control input.

The RMS of the velocity of the error signal is depicted in Figure 7b. The velocity also shows a significant decrease for higher refresh rates [$F(4, 36) = 8.028$, $p < 0.001$], which is determined to be primarily a linear trend that explains 89% of the variance [$F(1, 9) = 19.386$, $p < 0.005$]. Figures 7a and 7b show that pilots were able to compensate for the error more effectively by reducing both the magnitude and the velocity of the error signal. Note that the means of the RMS of the error only cover 2.4 to 2.8 deg of visual angle. The mean RMS values of the velocity are between 7 and 8 deg/s, sufficiently high enough to induce significant spatio-temporal aliasing artifacts.[3]

Figure 8 depicts the mean histogram of the error velocity signal. The mean histogram is calculated by averaging the histograms of the time-domain data from every subject and every condition. The histogram data are approximated by a normal distribution ($\mu = 0$,$\sigma = 7.735$). Vertical lines indicate the one and two standard deviation distances from the mean, and the percentage of data between these lines. From Figure 8 it can be concluded that 32% of the time the velocity of the visual stimulus, that is, the velocity of the error line, was above 7.735 deg/s. Comparing this to the results of Watson et al. in Figure 3 shows that for all conditions aliasing artifacts should be present. Note, however, that this only serves as an indication, as a different task and experiment setup were used to acquire these results.

Figure 9 depicts the RMS of the control signal. The control effort remains constant for all conditions, that is, no significant effect was found [$F(4, 36) = 0.454$, $p > 0.05$].

B. Pilot Control Behavior

The parameters of the pilot model [Eq. (5)] were estimated by minimizing a frequency-domain criterion. This criterion was a weighted difference between the pilot model open-loop frequency response function and an autoregressive exogenous (ARX) model frequency response estimate of the open-loop describing function.[16,17] For every condition of every subject the ARX model estimate was calculated using the averaged time-domain data from eight runs to reduce the influence of the pilot remnant. The time delay of the pilot model was included using a fifth-order Padé approximation.

The variance accounted for (VAF) is a measure of how well the linear pilot model can explain the measured experimental data. The VAF highly depends on the control strategy of the pilot, that is, the linearity of the pilot's control action, and the fidelity of the model. For the estimated pilot models, the VAF of the pilot control signal, calculated using the averaged data, was around 90% for eight of the ten pilots, a value also found in previous experiments.[16] For two subjects the VAF was slightly lower at around 83%.

Figure 10 depicts the frequency responses of the pilot model and the open-loop for a single pilot. For clarity, only the frequency responses of the lowest and highest tested refresh rates (60 and 120 Hz) are given. A change in control strategy can be seen between the two conditions. From the pilot model and open-loop magnitude plots (Figures 10a and 10c) an increase in pilot gain can be seen for the higher refresh rate. Furthermore an increase in neuromuscular frequency can be observed by the slight shift of the neuromuscular peak to the right. From the phase plots (Figures 10b and 10d) a decrease in effective time delay can be seen. The frequency responses for the remaining conditions follow the same trend and their magnitude and phase are located between the depicted extremes in Figure 10. For all pilots similar effects of refresh rate on the pilot model and open-loop frequency responses were observed.

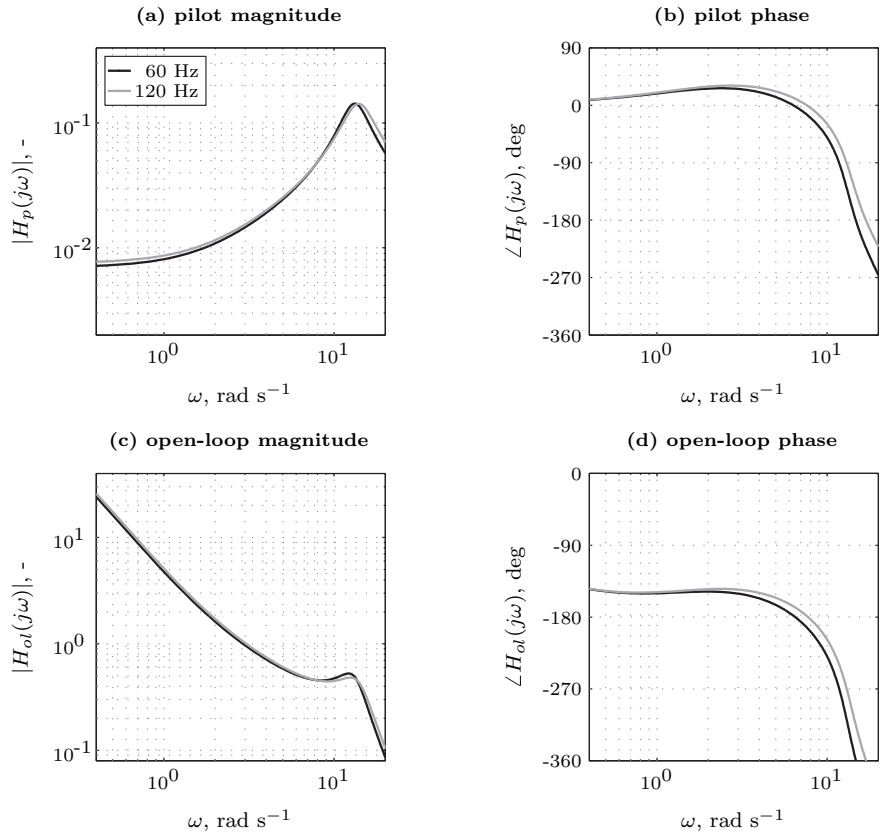

Figure 10. Pilot and open-loop frequency response functions (pilot 2).

The observed change in pilot control strategy can be quantified by inspecting the pilot model parameters of Eq. (5). The means and 95% confidence intervals of the estimated pilot model parameters are shown in Figure 11. As could be observed from the calculated frequency response functions in Figure 10, an increase in visual gain for increasing refresh rates can be seen in Figure 11a. This increase in visual gain is significant [$F(4, 36) = 3.351$, $p < 0.05$] and polynomial contrasts indicate that the trend is primarily linear and accounts for 89% of the variance [$F(1, 9) = 21.691$, $p < 0.001$].

Figure 11c indicates a significant decrease in equivalent visual time delay when the refresh rate increases [$F(4, 36) = 16.103$, $p < 0.001$]. This decreasing trend is found to be completely linear, as the linear contrast explains 100% of the variance [$F(1, 9) = 60.981$, $p < 0.001$]. The dashed lines show the part of the visual time delay trend that might be explained by the fact that the visual display updates at a higher refresh rate (visual information on the error is available sooner). As can be observed, the actual trend decreases much faster, most likely due to the decrease in spatio-temporal artifacts as the refresh rate increases.

An increase in neuromuscular frequency for increasing refresh rate is observed from Figure 11e. This effect is significant [$F(4, 36) = 5.686$, $p < 0.001$] and the trend is primarily linear, explaining 75% of the variance [$F(1, 9) = 10.785$, $p < 0.01$]. From Figures 11b and 11d, no significant effects were observed for the visual lead time constant [$F(4, 36) = 1.476$, $p > 0.05$] or the neuromuscular damping [$F(4, 36) = 1.007$, $p > 0.05$].

In the frequency domain, pilot performance is characterized by properties of the open-loop frequency response, such as the crossover frequency and phase margin (Figure 12). Figure 12a depicts the mean and 95% confidence intervals for the crossover frequency for every condition. An increase in crossover frequency can be observed for increasing refresh rates. This is a significant effect [$F(4, 36) = 3.173$, $p < 0.05$] and the trend is found to be primarily linear, explaining 72% of the variance [$F(1, 9) = 31.960$, $p < 0.001$]. A similar increasing trend appears for the phase margin in Figure 12b, suggesting increased stability margins when the refresh rate is increased. However, this trend is not found to be significant [$F(4, 36) = 1.560$, $p > 0.05$].

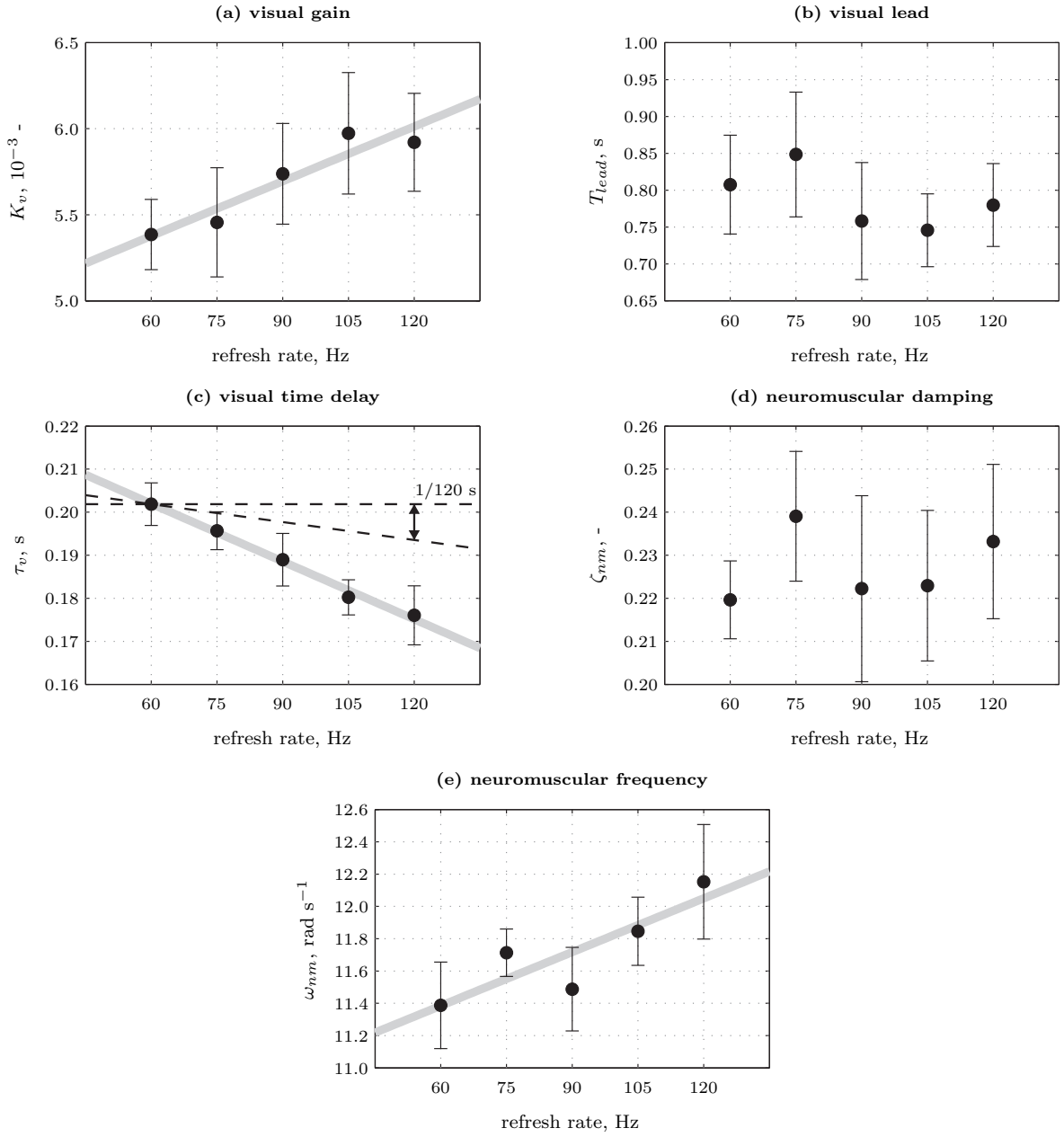

Figure 11. Means and 95% confidence intervals of the model parameters. The data are corrected for between-subject variability. Significant linear trends are indicated by grey lines.

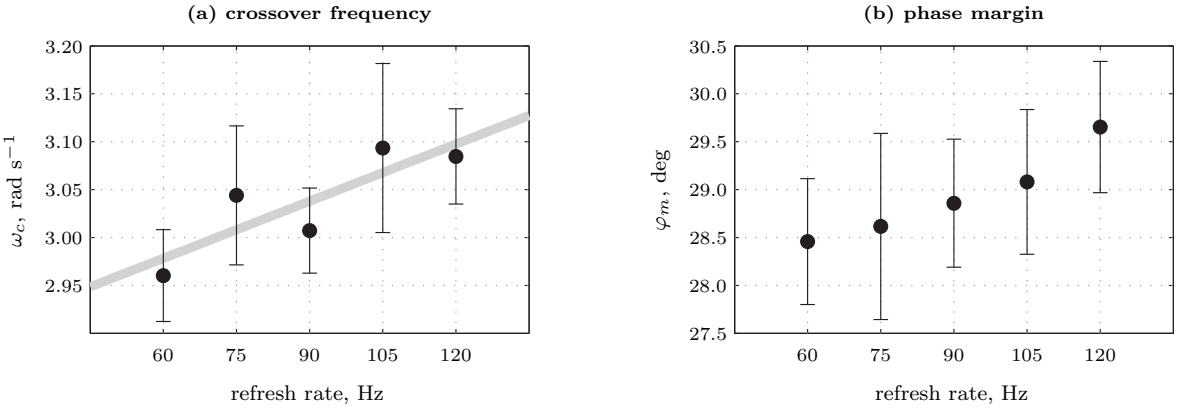

Figure 12. Means and 95% confidence intervals of crossover frequency and phase margin. The data are corrected for between-subject variability. Significant linear trends are indicated by grey lines.

V. Discussion

For a given human visual temporal sensitivity, refresh rate, and maximum spatial frequency, the intensity of spatio-temporal artifacts is dependent on the velocity of the visual stimulus. In this experiment the velocity of the stimulus – the line indicating the error on the compensatory display – is not constant and is dependent on the control action of the pilot. This means that, theoretically, for increasing levels of target-tracking performance, the velocity of the error can be reduced below the velocity threshold where spatio-temporal aliasing becomes apparent. However, Figure 7b indicates that the mean RMS of the error velocity is high enough for all conditions to induce aliasing artifacts. Furthermore, the histogram of the velocity of the error (Figure 8) also indicates velocities above 8 deg/s for a significant part of the experiment run. This is also confirmed by observations during the experiment; all pilots indicated the visibility of aliasing artifacts for all conditions. Furthermore, although some pilots were able to observe visible differences between conditions in terms of the intensity of the aliasing artifacts, they were generally not able to indicate whether the current condition had a lower or higher refresh rate compared to other conditions.

The results of the experiment indicate a significant change in pilot control behavior when increasing the refresh rate of the display. This change in control strategy was captured by a change in the estimated pilot model parameters. The visual gain and neuromuscular frequency both increased when the refresh rate was increased, while the visual time delay decreased (Figure 11). Similar trends in visual gain, time delay, and neuromuscular frequency have been observed in many experiments on the effects of degrading visual information on pilot control behavior.[11,12,14,18] However, the hypothesized increase in the visual lead time constant for an increase in refresh rate – that is, an increase in the amount of lead generated by the pilot – was not observed in this experiment. Tentatively, this may be explained by the fact that the visual lead time constant is primarily dictated by the requirement to generate lead to compensate for the double-integrator dynamics at higher frequencies. An increase in visual lead time constant for higher refresh rates is not necessary as the controlled dynamics are constant in the experiment. Other simulated piloting tasks where performance is more dependent on the perception of visual motion – such as an autorotative descent and landing,[6] or a yaw capturing task in a helicopter[19] – could be more suitable to reveal a significant change in the pilot's ability to generate lead as refresh rate varies. However, the modeling of pilot control behavior is significantly more difficult for such tasks, as control behavior is more nonlinear.

The decrease in visual time delay observed in Figure 11c could be a direct result of the higher refresh rate of the CRT monitor (visual information on the error is updated at a higher rate), as opposed to a decrease in spatio-temporal aliasing artifacts at these higher refresh rates. This would mean the observed results would be wrongly assigned to the effects of spatio-temporal aliasing. However, as also depicted in Figure 11c, the decrease in visual time delay as a direct result of the increased refresh rate from 60 to 120 Hz can only be 1/120 s. The observed decreasing trend in the estimated visual time delay is much steeper and can therefore not be assigned only to the increased refresh rate, but is likely to have been also caused by a decrease in aliasing artifacts.

The significant change in pilot control behavior observed for an increase in refresh rate resulted in an increase in target-tracking performance. This was indicated by a significant decrease in RMS of the error

and error velocity (Figure 7). Furthermore, an increase in crossover frequency was observed in Figure 12a, indicating increased performance in attenuation of the error signal in the frequency domain.

While the observed effects in the dependent measures noted here were modest, they were limited by the experimental apparatus to a limited field of view. The field of view limited image motion as the stimulus was not allowed to go off the screen. Furthermore, a forcing function that induces faster image motions would be likely to introduce crossover regression. In an actual simulation there can be significant amounts of image motion. Particularly pitch and yaw produce uniform image motion, while roll motion creates significant image motion at a distance from the roll axis. These rotational movements create the potential for spatio-temporal aliasing artifacts to become quite salient. Next steps are to look at the effect of refresh rate for more realistic tasks with a larger field of view.

All the observed significant trends in the data are found to be highly linear according to polynomial contrast analyses. However, it can be expected that when the limits of human temporal sensitivity and spatial acuity are reached, a further increase in refresh rate would not have any effect. When approaching these limits of human visual perception, the trends are not expected to be linear, but to curve to a limit value. A previous experiment found that a refresh rate of approximately 240 Hz eliminates aliasing artifacts completely.[5,13] In the current experiment the maximum refresh rate of 120 Hz was the highest refresh rate that was supported by the CRT monitor. However, to investigate the trends near the limits of human visual perception, future experiments on the effects of spatio-temporal aliasing on pilot performance in active control tasks should also include refresh rates in excess of 120 Hz if allowed by the display device.

During the experiment, pilots were asked to fixate in the middle of the CRT monitor. However, there were no means available to verify this. It has been shown that the sensitivity to spatio-temporal aliasing depends on whether the image motion is tracked with pursuit eye movements, or whether the eyes are fixated on a fixed point. Aliasing artifacts are much more evident in fixation than pursuit.[5] In future experiments an eye tracker could be used to verify that subjects are indeed fixating on the instructed point. Furthermore, as most piloting tasks require pilots to engage in pursuit eye movements when viewing a simulated out-the-window display, more research is needed on the effects of aliasing artifacts on pilot performance in active control tasks with pursuit eye movements.[13]

VI. Conclusions

Ten general aviation pilots participated in an experiment to determine the effects of spatio-temporal aliasing on pilot performance and control behavior in an active control task. Pilots performed a target-tracking task, minimizing the error between the desired and actual controlled system state. In five experimental conditions, the refresh rate of the CRT monitor depicting a compensatory display was varied between 60 and 120 Hz.

Pilot control behavior was significantly affected by a decrease in spatio-temporal aliasing artifacts as the display refresh rate increased. The visual gain and neuromuscular frequency significantly increased and the visual time delay decreased following a linear trend. This change in control strategy allowed for significant better target-tracking performance and an increase in crossover frequency associated with an increase in refresh rate.

References

[1]Sweet, B. T. and Hebert, T. M., "The Impact of Motion-Induced Blur on Out-The-Window Visual System Performance," *Proceedings of the IMAGE 2007 Conference, Scottsdale (AZ)*, July 2007.

[2]Sweet, B. T. and Giovannetti, D. P., "Design of an Eye Limiting Resolution Visual System using Commercial-off-the-shelf Equipment," *Proceedings of the AIAA Modeling and Simulation Technologies Conference and Exhibit, Honolulu (HI)*, No. AIAA-2008-6847, 18–21 Aug. 2008.

[3]Watson, A. B., Ahumada, Jr., A. J., and Farrell, J. E., "Window of Visibility: A Psychophysical Theory of Fidelity in Time-Sampled Visual Motion Displays," *Journal of the Optical Society of America A*, Vol. 3, No. 3, March 1986, pp. 300307.

[4]Winterbottom, M., Gaska, J., Geri, G., and Sweet, B., "Evaluation of a Prototype Grating-Light-Valve Laser Projector for Flight Simulation Applications," *SID International Symposium Digest of Technical Papers*, Vol. 39, May 2008, pp. 911–914.

[5]Kuroki, Y., Nishi, T., Kobayashi, S., Oyaizu, H., and Yoshimura, S., "Improvement of Motion Image Quality by High Frame Rate," *SID International Symposium Digest of Technical Papers*, Vol. 37, June 2006, pp. 14–17.

[6]Dearing, M., Schroeder, J., Sweet, B., and Kaiser, M., "Effects of Visual Texture, Grids, and Platform Motion on Unpowered Helicopter Landings," *Proceedings of the AIAA Modeling and Simulation Technologies Conference and Exhibit, Montreal, Canada*, No. AIAA-2001-4251, Aug. 6–9 2001.

[7]McRuer, D. T., Graham, D., Krendel, E. S., and Reisener, W., "Human Pilot Dynamics in Compensatory Systems.

Theory, Models and Experiments With Controlled Element and Forcing Function Variations," Tech. Rep. AFFDL-TR-65-15, Wright Patterson AFB (OH): Air Force Flight Dynamics Laboratory, 1965.

[8]Zaal, P. M. T., Pool, D. M., Mulder, M., and van Paassen, M. M., "Multimodal Pilot Control Behavior in Combined Target-Following Disturbance-Rejection Tasks," *Journal of Guidance, Control, and Dynamics*, Vol. 32, No. 5, Sept.–Oct. 2009, pp. 1418–1428.

[9]Groot, T., Damveld, H. J., Mulder, M., and van Paassen, M. M., "Effects of Aeroelasticity on the Pilots Psychomotor Behavior," *Proceedings of the AIAA Atmospheric Flight Mechanics Conference and Exhibit, Keystone (CO)*, No. AIAA-2006-6494, 21–24 Aug. 2006.

[10]McRuer, D. T. and Jex, H. R., "A Review of Quasi-Linear Pilot Models," *IEEE Transactions on Human Factors in Electronics*, Vol. HFE-8, No. 3, 1967, pp. 231–249.

[11]Li, L., Sweet, B. T., and Stone, L. S., "Effect of Contrast on the Active Control of a Moving Line," *Journal of Neurophysiology*, Vol. 93, No. 5, May 2005, pp. 2873–2886.

[12]Li, L., Sweet, B. T., and Stone, L. S., "Active Control With an Isoluminant Display," *IEEE Transactions on Systems, Man, and Cybernetics; Part A: Systems and Humans*, Vol. 36, No. 6, Nov. 2006, pp. 1124–1134.

[13]Sweet, B. T., Stone, L. S., Liston, D. B., and Hebert, T. M., "Effects of Spatio-Temporal Aliasing on Out-The-Window Visual Systems," *Proceedings of the IMAGE 2008 Conference, St. Louis (MO)*, June 2008.

[14]Zaal, P. M. T., Nieuwenhuizen, F. M., Mulder, M., and van Paassen, M. M., "Perception of Visual and Motion Cues During Control of Self-Motion in Optic Flow Environments," *Proceedings of the AIAA Modeling and Simulation Technologies Conference and Exhibit, Keystone (CO)*, No. AIAA-2006-6627, 21–24 Aug. 2006.

[15]Loftus, G. R. and Masson, M. E. J., "Using Confidence Intervals in Within-Subject Designs," *Psychonomic Bulletin & Review*, Vol. 1, No. 4, 1994, pp. 476–490.

[16]Nieuwenhuizen, F. M., Zaal, P. M. T., Mulder, M., van Paassen, M. M., and Mulder, J. A., "Modeling Human Multichannel Perception and Control Using Linear Time-Invariant Models," *Journal of Guidance, Control, and Dynamics*, Vol. 31, No. 4, July–Aug. 2008, pp. 999–1013.

[17]Jex, H. R., Magdaleno, R. E., and Junker, A. M., "Roll Tracking Effects of G-vector Tilt and Various Types of Motion Washout," *Fourteenth Annual Conference on Manual Control*, University of Southern California, Los Angeles (CA), April 25–27 1978, pp. 463–502.

[18]Sweet, B. T. and Kaiser, M. K., "Modeling of Perception and Control of Attitude with Perspective Displays," *Proceedings of the AIAA Modeling and Simulation Technologies Conference and Exhibit, San Francisco (CA)*, No. AIAA-2005-5891, 15–18 Aug. 2005.

[19]Ellerbroek, J., Stroosma, O., Mulder, M., and van Paassen, M. M., "Role Identification of Yaw and Sway Motion in Helicopter Yaw Control Tasks," *Journal of Aircraft*, Vol. 45, No. 4, July–Aug. 2008, pp. 1275–1289.